

Stress Concentration Factor in a Functionally Graded Material Plate around a Hole

Javad Jafari Fesharaki^{1*}, Seyed Ghasem Madani², Davood Seydali¹

¹Department of Mechanical Engineering, Najafabad Branch, Islamic Azad University, Najafabad, Iran

²Department of Mechanical Engineering, Faculty of Engineering, University of Kashan, Kashan, Iran

*Email of Corresponding Author: jjafari.f@gmail.com

Received: February 3, 2017; Accepted: May 24, 2017

Abstract

Stress concentration factors have been examined in a functionally graded material (FGM) plate with central holes in different shapes in this essay. The material properties change along the thickness of plate. ABAQUS software has been utilized for modeling of problem in which subroutine of ABAQUS sub-program was used for modeling of the targeted material. The considering shapes for hole in plate are circular and elliptical in which stress concentration factors have been studied in different modes in respective of ellipse diameters. Similarly, stress concentration factors have been analyzed in the plate for various coefficients of FGM function. The results show that changes in material properties and the shape of hole in plate affect the stress concentration factor around the hole. An experiment was implemented to determine verification of results from Finite Element Method (EFM).

Keywords

Stress Concentration Factor, Functionally Graded Material, Finite Element, Subroutine

1. Introduction

Functional graded materials are of materials whose properties are changed functionally in a certain direction. Such changes in certain direction produce specific properties, including controlling the stress component (stress management). Such excellent properties of FGM have attracted researchers and scientists to study on and to make use of these materials in various industries, including aerospace, materials, chemistry and other fields. Hufenbach et al. [1] obtained an analytical method for determining the stress concentration factor of the composite plate with an elliptic hole. In this study, the stress concentration at different angles position of the ellipse relative to the horizontal axis is investigated. In this study, using the least squares method for the outer boundary of the stress concentration in each layer is obtained. Kubair and Bhanu-Chandar [2] presented the stress concentration factor on a plate with a hole circle under uniaxial tension. The property in homogeneity material effect on the amount of stress around the hole was investigated. The results show that, when the modulus factor of elasticity increases, the stress concentration factor around the hole reduces. Rezaeepazhand and Jafari [3] investigated the stress concentration factor at the metal plates with different shapes in the center of the plate to cut the Flow tension. The purpose of this study is to provide a method for central cutout, in a plate under tension using a different shape in the center. To conclude, the stress concentration factor can be used in different shape in the center of

the hole, with cutout significantly reduced. Yang et al. [4-6] conducted an analysis of a plate FGMP with a hole circle and studies have shown that the radial Young's modulus, a large impact on reducing the stress and Poisson's ratio effect on reducing stress is low. They also have a similar study, the stress concentration at a finite plate made of FGM performed with a circular hole performed. Amount of stress concentration factor at the hole, according to amount power, material plate and different size plates were studied. They also work the same; Non-Axisymmetric thermal stress plate with holes was examined. Jabbari et al. [7-8] presented thermal and mechanical stress analysis of a cylinder of material FGM. The FGM material in the radial direction is graded. Bodaghi and saidi [9] examined the stability of rectangular plates made of functionally graded materials in a non-uniform loading on elastic foundation. An analytical solution for the buckling of plates FGM using Levy-type solution is obtained. Bouiadjra et al. [10] presented Four-Variable theory for thermal buckling of sheets made of functionally graded materials. Gosh and kanoria [11] investigated thermo elastic response of a hollow sphere of material FGM, based on the theory of thermo-elasticity studied. The results show that the thermo-physical properties of the material and the thickness of the sphere are very impressive. Chen et al. [12] studied the stress analysis on a plate with a hole in the functionally graded materials under load symmetric. They concluded that radial elastic modulus is highly effective in reducing stress. Shen and Noda [13] presented buckling analysis of a cylinder made of F-GM, under external pressure with a piezoelectric actuator that produces the electricity. The cylinder is located in a thermal environment and the results show that changes in temperature and power index of the FGM has significant impact on reducing buckling, but piezoelectric voltage did not have little impact on reducing buckling cylindrical FGM. Liew et al. [14] investigated thermal analysis of a cylinder of material FGM and concluded that the combination matter on thermal stress on cylinder will have a significant impact. Ootao et al. [15] obtained an optimal combination of FGM to control thermal stress in a cylinder using neural network approach. Han et al. [16] worked on the analysis of transient waves in a cylinder of functionally graded material. Abrinia et al. [17] presented an analytical solution for the evaluation of thermal stress in a cylindrical FGM. Tutuncu and Temel [18] obtained a new method for the analysis cylinders of FGM material. The material is assumed to be functionally graded in the radial direction and Young's modulus and Poisson's ratio as the desired function of radius change. In this paper, the stress concentration factor in a sheet with a central hole in different shapes is investigated. FGM material is distributed in line with the sheet's thickness, and to do that, a Python code has been developed in the software ABAQUS and the stress concentration factor has been introduced in various forms of hole, including circular hole and elliptical hole with different diameters' ratio. The stress concentration factor is investigated in each of these forms in different exponential coefficients of FGM and the results will be presented. A practical test is performed to validate.

2. Modeling

A sheet of 200, 100, and 1 mm in length, width and thickness was selected, respectively, as the problem. FGM is converted in terms of properties as a function of underlying layer with modulus of elasticity $10e5$ into the upper layer with modulus of elasticity $200e5$. Exponential coefficients of FGM are changed for all forms as shown in Table (1).

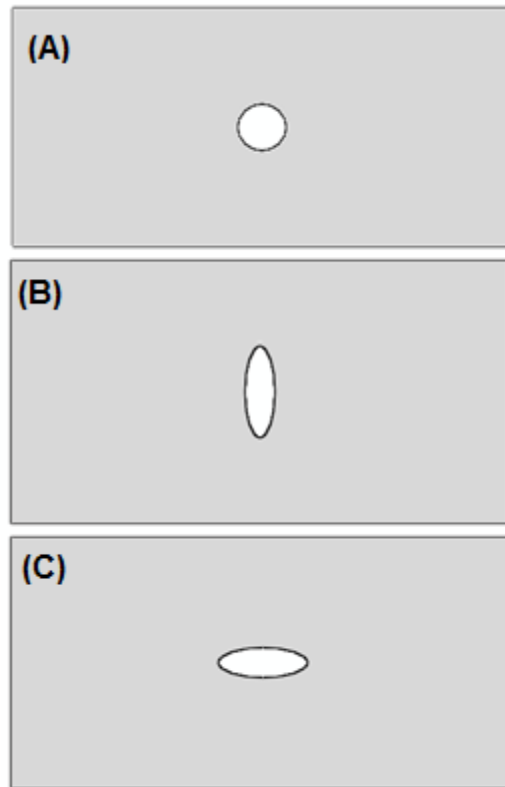


Figure1. Schematic problem

Table1. Change the properties of FGM

N	-0.2	-0.4	-0.6	-0.8	0	0.2	0.4	0.6	0.8
---	------	------	------	------	---	-----	-----	-----	-----

3. Finite Element Simulation

The simulation in this paper was performed by ABAQUS finite element software. The problem is examined for three different modes and the results are presented -0.1 Sheet with a central circular hole in a radius of 10 mm -0.2 Sheet with an elliptical hole with different diameters' ratio -0.3 presenting the results for the same exponential coefficients of FGM for circular hole and elliptical one with different diameters ratio.

4. Results and Discussion

After the simulation, the results will be presented in the form of applied charts.

First case: Results for sheet perforated with central circular holes:

As shown in Figure (1-A), the different exponential coefficients of FGM are provided for the case where the hole is circular. Figure (2) depicts the stress in the circular hole in the thickness of the sheet for the different exponential coefficients.

As can be seen in Figure (2), the stress in the lower layer (with a thickness of zero) is equal to 3.7 Mpa at the coefficient of zero ($n = 0$), and it increases from the coefficient of zero toward the

negative coefficients, and the curves are descending from the thickness of 0 to 0.5 mm. in which the stress is reduced compared to the initial thickness. But in positive exponential coefficients, the more we move toward the positive coefficients from the coefficient of zero, the more the stress is reduced in the initial thickness and as it can be seen, the curve for the positive exponential coefficients is reverse to the negative ones, i.e. there is an ascending curve from the thickness of 0 to 0.5 mm. and the stress increases in them. The curves intersect at the thickness of 1.25 mm. and from that point on the curves continue uniformly.

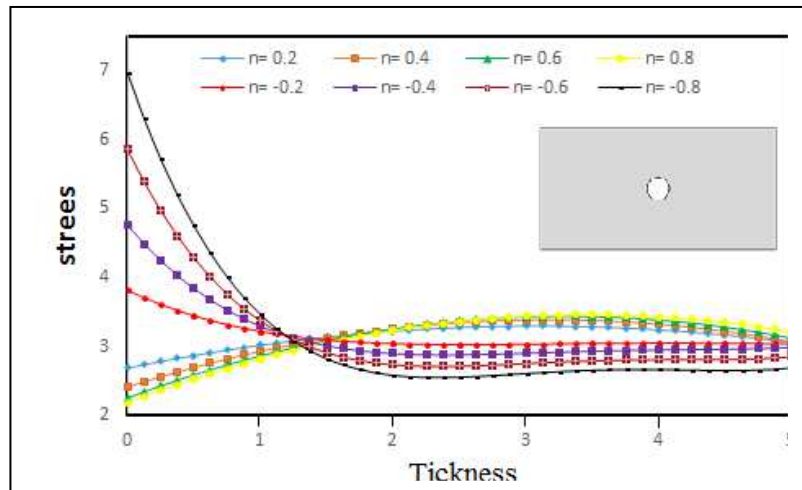


Figure2. Stress curve for case circle

Second case: Results for sheet perforated with elliptical holes with different diameters’ ratio:

As shown in Figure (1-B) and (1-C), different FGM exponential coefficients are given for the case in which the hole is oval-shaped and of different diameters’ ratio. Different diameters’ ratio is given in Table (2). Figure (3) shows the graph of stress in the sheet thickness for different exponential coefficients at the diameters’ ratio of $D_1/D_2=2$. At the lower layer, the exponential coefficient -8 shows the most stress, and the stress is reduced in the lower layer from this point to the exponential coefficient 0. From the exponential coefficient 0 toward the positive ones, the stress concentration is reduced. And at the coefficient +8, it reaches to its minimum value. The negative exponential coefficient shows the descending trend and the positive ones follows an ascending trend and it leads them to intersect at the thickness of 1.8 mm. From the intersection point on, the slope of curves shifts resulting in a re-intersection of curves at the thickness of 0.5 mm.

Figure (4) shows the diameters’ ratio ($D_1/D_2=3$) for the stress in the sheet thickness. As shown, the stress decreases from the exponential coefficient 0 to the negative ones at the thickness of 0 mm, and the lowest stress is related to the coefficient -8 with value of 2.15 Mpa. For the exponential coefficients +8, the greatest stress of 5.64 Mpa was seen at the lower layer. The stress is reduced from the coefficient +8 toward the one of 0 mm. The graphs are descending for the positive coefficients and they are ascending for the negative ones. It leads them to intersect at the thickness of 1.65 mm. and from the intersection point on; their slope is changed to re-intersect at the thickness of 0.5 mm. As it can be seen, the diameter ratio 3 behaves exactly the opposite of the diameter ratio 2.

Figure (5) shows the stress at the sheet thickness for the different exponential coefficients for the diameter ratio $D_2/D_1=2$. As shown, the most stress concentration for the positive exponential coefficients is observed at the coefficient of 0.2. The coefficient of stress concentration is reduced toward the positive coefficients until the lowest stress is met at the thickness of 0 mm. for the coefficient 0.8. Among the negative coefficients, -8 show the most stress. The graphs are ascending for the positive exponential coefficients and they are descending for the negative exponential coefficients. The curves intersect at the thickness of 1.6 mm, and then they shift afterward to re-intersect at the thickness of 4.8 mm. At the thickness of 0.5 mm, the exponential coefficient of +8 shows again the lowest stress.

Figure (6) depicts the graph of the diameters' ratio ($D_2/D_1=3$) for the stress at the thickness of the sheet. As shown, the graph of the coefficient ($n=0$) is constant. At the thickness of 0 mm, the lowest concentration of stress is for the coefficient ($n=0.8$) and the highest one for the coefficient ($n=-0.8$). The graphs for the positive coefficients are ascending and the ones for the negative coefficients are descending. It leads the curves to intersect at the thickness of 1.5 mm, and then they changes in course and re-intersect at the thickness of 4.7 mm.

Table2. The ratio of diameters

$D_1 / D_2(\text{mm})$	$D_2 / D_1(\text{mm})$
2	2
3	3

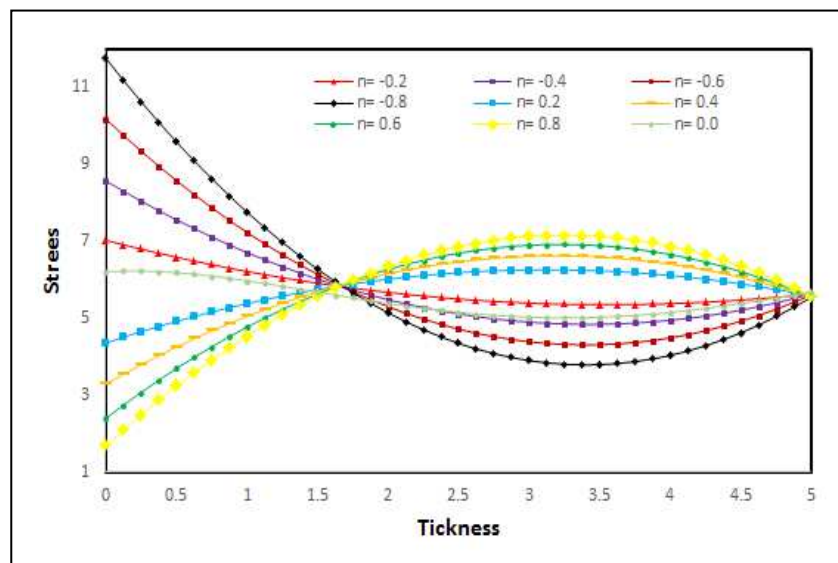


Figure3. Stress concentration for diameter ratio $d_1/d_2=2$

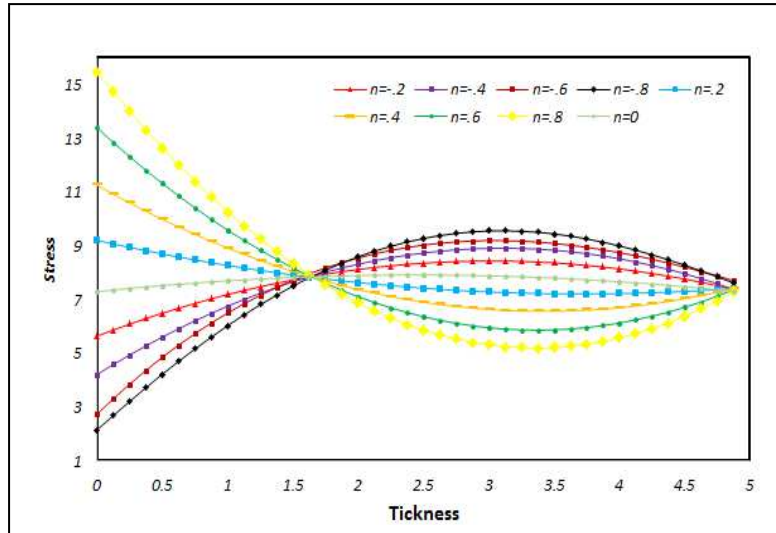


Figure4. Stress concentration for diameter ratio $d_1/d_2=3$

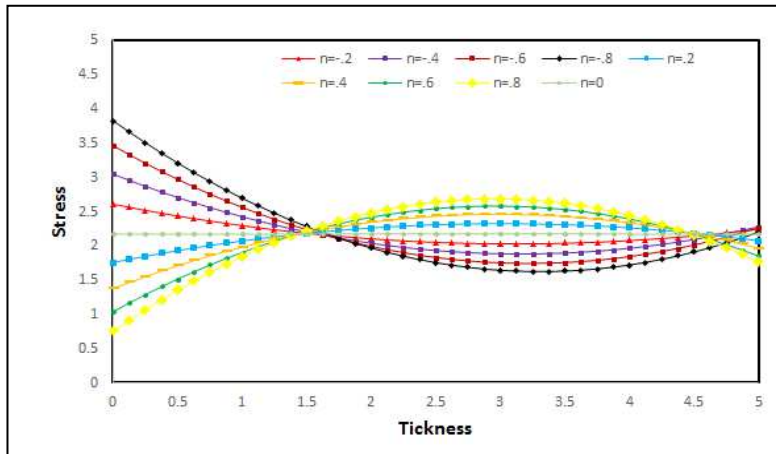


Figure5. Stress concentration for diameter ratio $d_2/d_1=2$

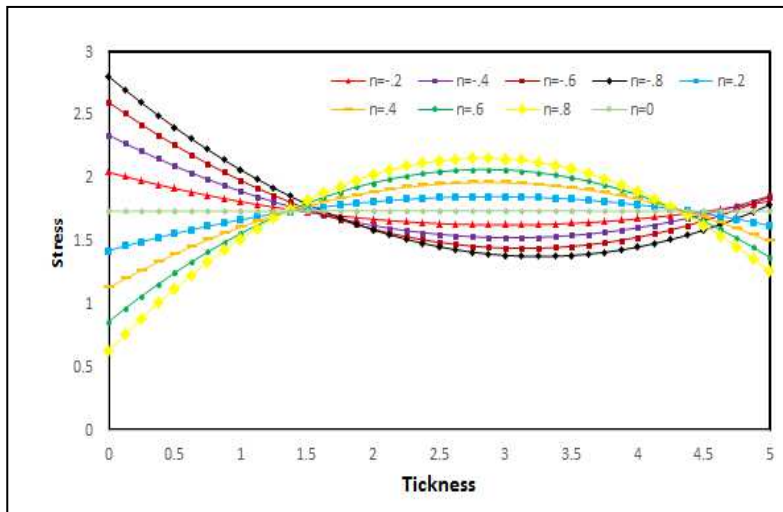


Figure6. Stress concentration for diameter ratio $d_2/d_1=3$

Third case: Results of the stress in the thickness of the sheet in fixed exponential coefficients for circular holes and elliptical ones with different diameters' ratio:

In these graphs and at the fixed exponential coefficients (n) for circular holes and elliptical ones with different diameters' ratio, the stress at the thickness of the sheet is drawn for the internal thickness of the sheet. The graphs of the stress at the thickness of the sheet for the coefficient ($n=-0.2$) is given in Figure (7). The graph for the circular holes show a descending slop and for the thickness of 1.8 on the slop is constant, and the most stress is revealed at the thickness 0. For the elliptical holes with the diameter ratio 2, the graph is descending and the lowest stress is at the thickness of 3.5 mm. For the elliptical holes with the diameter ratio 3, the lowest stress is at the thickness of 0 mm, and the graph is ascending and the most stress is at the thickness of 3 mm. Both graphs for the elliptical holes with the diameter ratios of 1/2 and 1/3 are descending, but the graph for the ratio of 1.2 shows more stress and are above the graph for the ratio of 1.3.

In Figure (8), the graphs are drawn for the coefficient ($n=-0.4$). The graphs for the circular holes and elliptical holes with the diameter ratios of 1/2 and 1/3 are descending and their most stress is at the thickness of 0. The graph for the diameter ratio 2 is descending and then it becomes ascending at the thickness of 3 mm. and shows the most stress at the thickness of 3.5 mm.. The graph for ($D1/D2=3$) is ascending and it changes its course at the thickness of 3 mm., and the lowest stress is seen at the thickness of 0, and the most stress is observed at the thickness of 3 mm., and the curves for the thickness ratio of 2 and 3 intersect at the thickness of 1.1 mm..

Figure (9) shows the graphs for the coefficient ($n=0.6$). The graph for the circular holes is descending but it is more inclined compared to two other cases. The graphs for the diameter ratios of 2 and 3 intersect at the thickness of 1.2 mm. The graph for the diameter ratio 3 of two graphs is circular and intersects the diameter ratio 1/2.

The stress for the various hole shapes in line with the thickness of the sheet is shown in Fig. (10) for the coefficient ($n=-0.8$). The graph for the circular hole is more inclined and changed from the stress 7 Mpa at the thickness of 0 to the stress 3 Mpa at the thickness of 1.8, and from this thickness on, the slope is constant. The graphs for the diameter ratios of 1/2 and 1/3 show a smooth slope, but the diameter ratios of 2 and 3 are very inclined and the stress is changed greatly in these ratios. Two graphs of the diameter ratios of 2 and 3 intersects at the thickness of 1.35 mm, and the graph for the diameter ratio of 3 intersects the graphs for the circular holes and the diameter ratios of 1/2 and 1/3.

In Figure (11), the graphs shows relatively a smooth slope for the coefficient ($n=0$), and not much stress changes are occurred here.

In Figure (12), it is shown that for the coefficient ($n=0.2$), the graphs are ascending for the circular holes and the diameter ratios of 1/3 and 1/2 for the ellipse with a smooth slope. The graph is in descending slope for the diameter ratio of 3 and is ascending for the diameter ratio of 2, and it changes its slope at the thickness of 3.3 mm, and the most stress is occurred at the point of changing the slope.

For the coefficient ($n=0.4$), the graphs for the diameter ratios of 3 and 2 intersect at the thickness of 3.3 mm, shown in Figure (13).

Figure (14) shows the graphs for the diameter ratios of 2 and 3 for the coefficient ($n=0.6$), intersecting at the thicknesses of 2.4 and 4.3 mm.

In Figure (15), for the coefficient ($n=0.8$), the graphs are ascending for the circular holes and the diameter ratios of $1/3$ and $1/2$, while the graph for the diameter ratio of 3 is inclined sharply and the difference of stresses at the thickness of 0 mm. and the one of 5 mm. is about 10 Mpa. The graphs for the diameter ratios of 3 and 2 intersect at the thicknesses of 2.1 mm. and 4.5 mm.

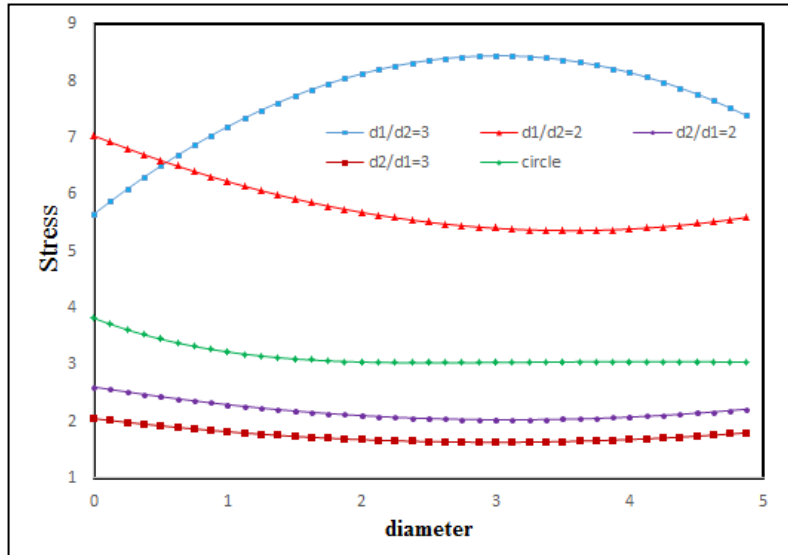


Figure7. Graph stress distribution for $n=-0.2$

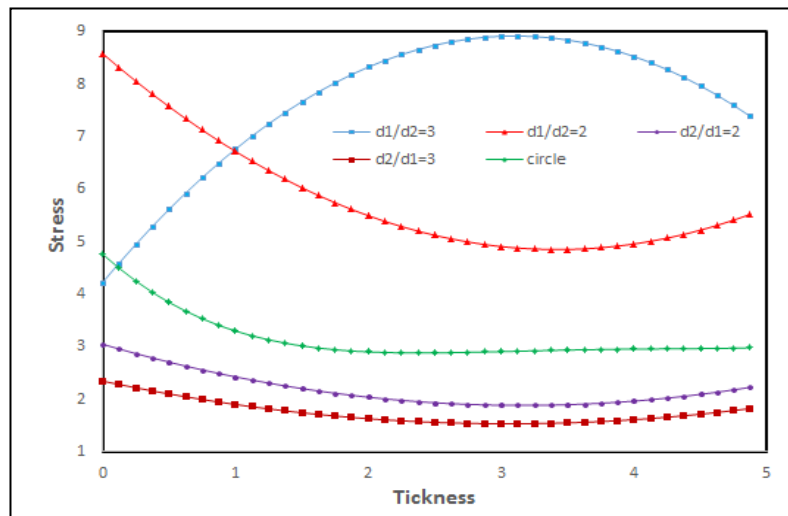


Figure8. Graph stress distribution for $n=-0.4$

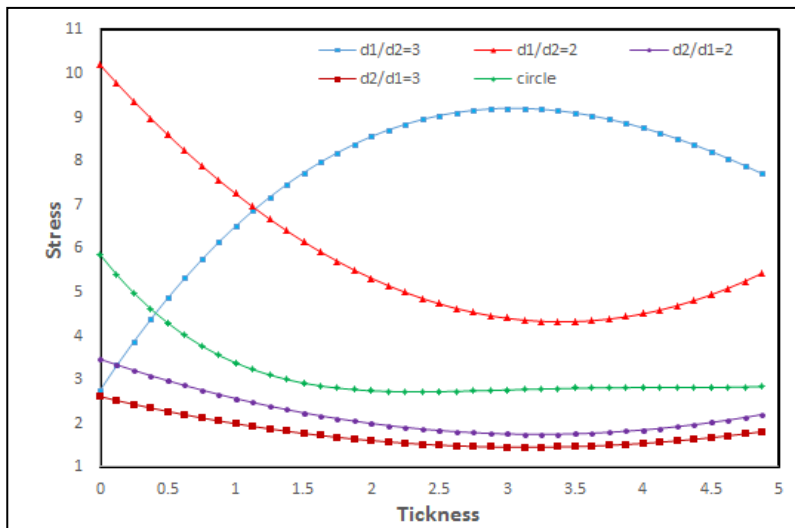


Figure9. Graph stress distribution for $n=-0.6$

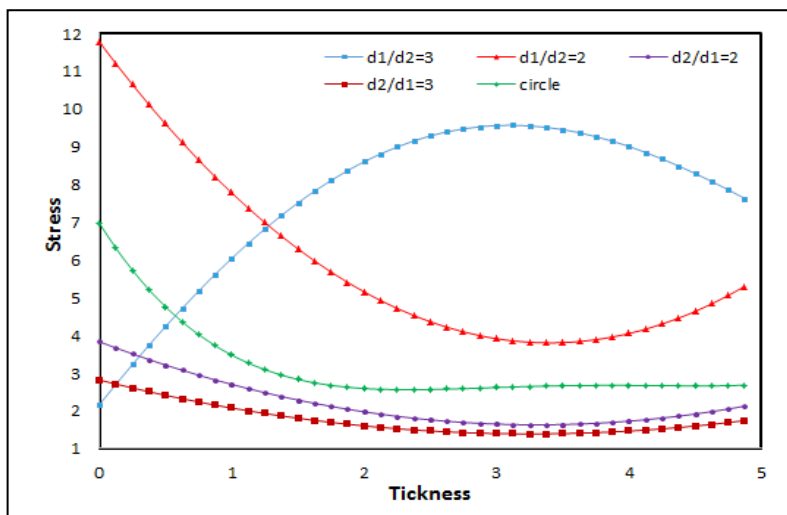


Figure10. Graph stress distribution for $n=-0.8$

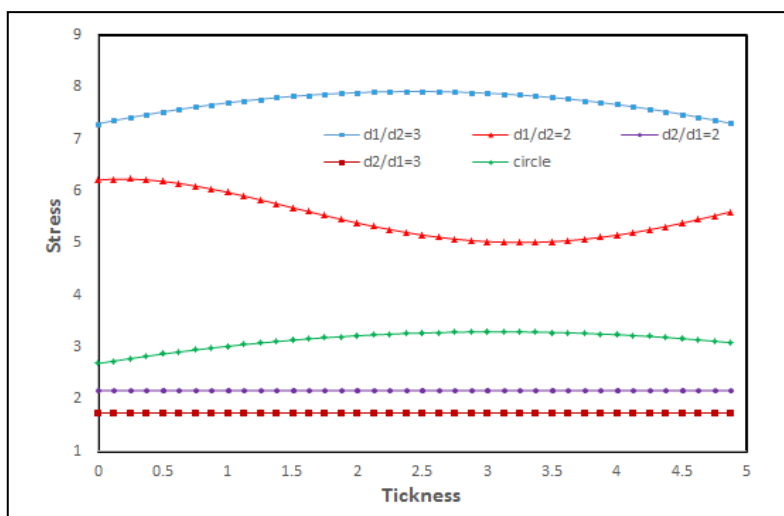


Figure11. Graph stress distribution for $n=0.0$

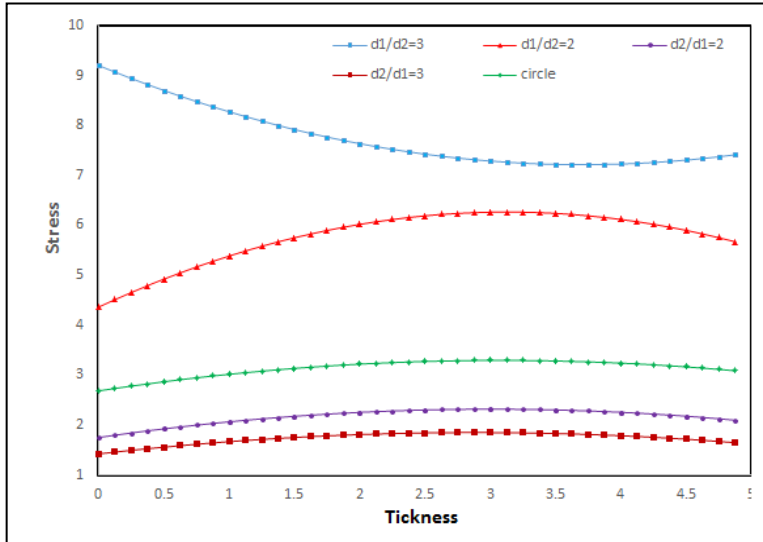


Figure12. Graph stress distribution for $n=0.2$

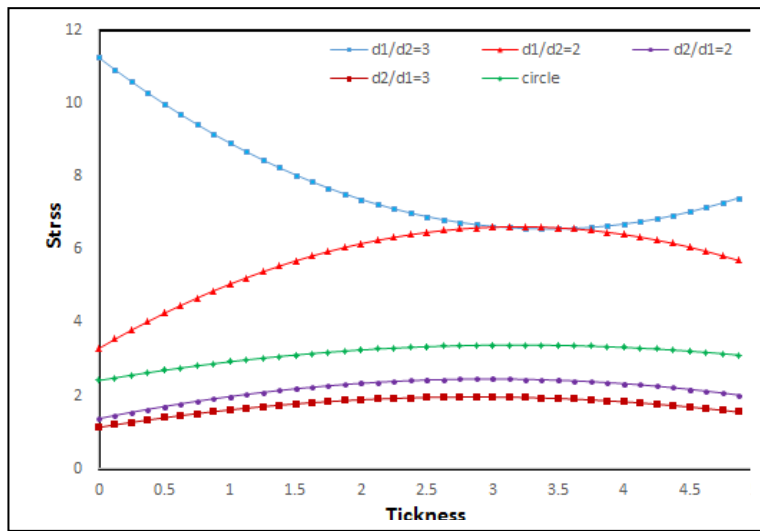


Figure13. Graph stress distribution for $n=0.4$

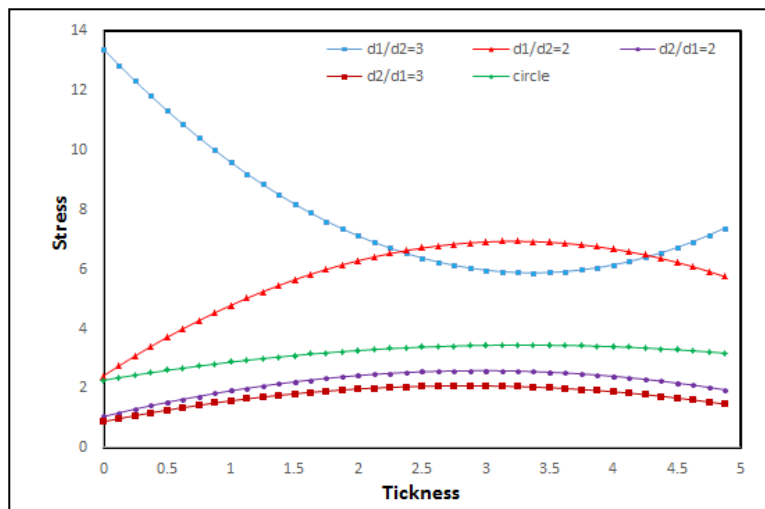


Figure14. Graph stress distribution for $n=0.6$

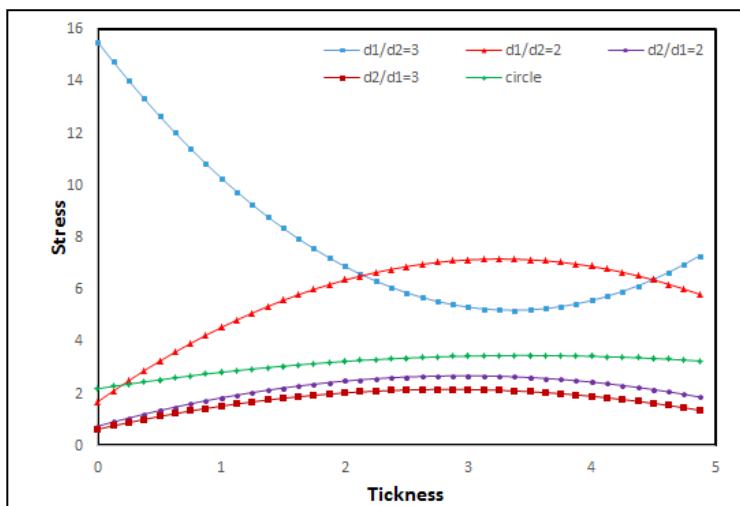


Figure15. Graph stress distribution for n=0.8

5. Laboratory Experiment

An experiment has been conducted for verification of FEM results as in Figure 16 where in this test a plate with circular hole was under tension force. Two strain-gauges are placed at above and below the hole to measure strain during experiment. The plate is made of a material for which FGM function is set to zero ($n=0$). As it is observed in Table 3, there is favorable compliance between results of FEM and the given experiment and small difference may be due to this fact that the strain-gauges have not been attached accurately at top and bottom of this hole.



Figure16. Experiment Test

Table3. Comparison of FEM and Experimental Results

Comparison of FEM and Experimental Results			
Strain	Analysis	Test	Error(%)
Sample	48.52e-6	46.12e-6	4.9%

6. Conclusion

In this essay, stress concentration coefficient has been analyzed in a plate with different shapes of hole in which the plate is made of FGM material. Diagrams of stress have been drawn at plate thickness for different modes in respective of diameter of hole as well as at different ratios of exponential FGM coefficient. These diagrams are used for achieving the minimum stress concentration factor around the hole. The results show that changes in shape of hole and material property of plate can affect the stress concentration factor around the hole in plate. An experimental test has been carried out for verification of results from FEM analysis that favorably complies with FEM analysis.

5. Reference

- [1] hufenbach, W., Gruber, B., Lepper, M., Gottwald, R. and Zhou, B. 2013. An Analytical Method for the Determination of Stress and Strain Concentrations in Textile-Reinforced GF/PP Composites with Elliptical Cutout and a Finite Outer Boundary and its Numerical Verification. *Archive of Applied Mechanics*. 83(1): 125-135.
- [2] Kubair, B. and Bhanu, Ch. 2008. Stress Concentration Factor Due to a Circular Hole in Functionally Graded Panels under Uniaxial Tension. *International Journal of Mechanical Sciences*. 50(4): 732-742.
- [3] Rezaeepazhand, J. and Jafari, M. 2010. Stress Concentration in Metallic Plates with Special Shaped Cutout. *International Journal of Mechanical Sciences*. 52(1): 96-102.
- [4] Yang, Q., Gao, C.-F. and Chen, W. 2001. Stress Analysis of a Functional Graded Material Plate with a Circular Hole. *Archive of Applied Mechanics*. 80(8): 895-907.
- [5] Yang, Q.-q. Gao, C.-F. and Chen, W.-T. 2011. Stress Concentration around a Circular Hole in a Functionally Graded Material Finite Plate, in *Proceeding of IEEE, Shenzhen, China*.
- [6] Yang, Q. and Gao, C.-F. 2010. Non-Axisymmetric Thermal Stress Around a Circular Hole in a Functionally Graded Infinite plate. *Journal of Thermal Stresses*. 33(4): 318-334.
- [7] Jabbari ,M., Bahtui, A. and Eslami, M. 2006. Axisymmetric Mechanical and Thermal Stresses in Thick Long FGM Cylinders. *Journal of Thermal Stresses*. 29(7): 643-663.
- [8] Jabbari, M., Bahtui, A. and Eslami, M. 2009. Axisymmetric Mechanical and Thermal Stresses in Thick Short Length FGM Cylinders. *International Journal of Pressure Vessels and Piping*. 86(5): 296-306.
- [9] Bodaghi, M. and Saidi, A. 2011. Stability Analysis of Functionally Graded Rectangular Plates under Nonlinearly Varying in-Plane Loading Resting on Elastic Foundation. *Archive of Applied Mechanics*. 81(6): 765-780.

- [10] Bouiadjra, M. B., Ahmed Houari, M. S. and Tounsi, A. 2012. Thermal Buckling of Functionally Graded Plates According to a Four-Variable Refined Plate Theory. *Journal of Thermal Stresses*. 35(8): 677-694.
- [11] Ghosh, M. and Kanoria, M. 2009. Analysis of Thermoelastic Response in a Functionally Graded Spherically Isotropic Hollow Sphere based on Green–Lindsay Theory. *Acta Mechanica*. 207(1-2): 51-67.
- [12] Chen, W.-T., Gao, C.-F. and Yang, Q.-q. 2008. Stress Analysis of a Functional Gradient Material Plate with a Circular Hole under Symmetric Loads, in *Proceeding of IEEE, Nanjing, China*.
- [13] Shen, H.-S. and Noda, N. 2007. Postbuckling of Pressure-Loaded FGM Hybrid Cylindrical Shells in Thermal Environments. *Composite Structures*. 77(4): 546-560.
- [14] Liew, K., Kitipornchai, S., Zhang, X. and Lim, C. 2003. Analysis of the Thermal Stress Behaviour of Functionally Graded Hollow Circular Cylinders. *International Journal of Solids and Structures*. 40(10): 2355-2380.
- [15] Ootao, Y. , Tanigawa, Y. and Nakamura. T. 1999. Optimization of Material Composition of FGM Hollow Circular Cylinder under Thermal Loading: a Neural Network Approach, *Composites Part B: Engineering*. 30(4): 415-422.
- [16] Han, X., Liu, G., Xi, Z. and Lam, K. 2001. Transient Waves in a Functionally Graded Cylinder. *International Journal of Solids and Structures*. 38(17): 3021-3037 .
- [17] Abrinia, K., Naei, H., Sadeghi, F. and Djavanroodi, F. 2008. New Analysis for the FGM Thick Cylinders under Combined Pressure and Temperature Loading. *American Journal of Applied Sciences*. 5(7): 852-859.
- [18] Tutuncu, N. and Temel, B. 2009. A Novel Approach to Stress Analysis of Pressurized FGM Cylinders, Disks and Spheres. *Composite Structures*. 91(3): 385-390.